Supporting Information

Dynamics of an ultrafast folding subdomain in the context of a larger protein fold

Caitlin M. Davis and R. Brian Dyer

1. Temperature dependent FTIR spectra of FBP28 1L were recorded to confirm that the peptide was folded

Please find the FTIR spectroscopy method in the methods section of the full paper. Temperature dependent FTIR of FBP28 1L are reported in Figure 1S.

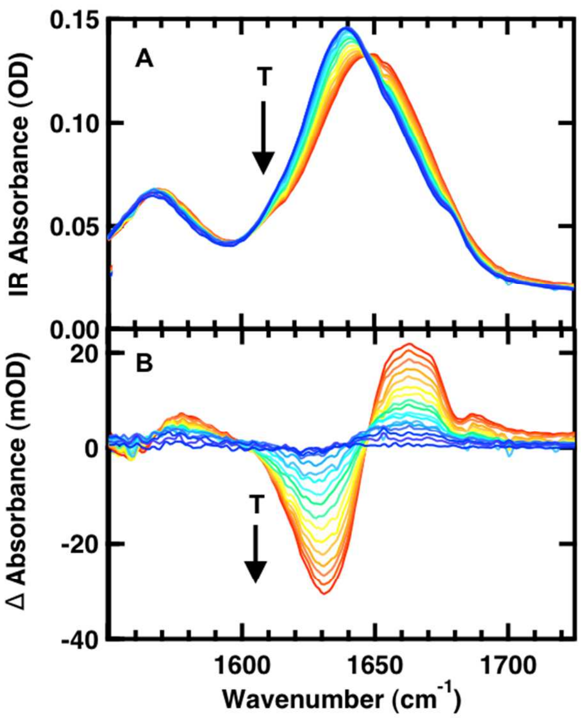

Figure 1S. Temperature dependent FTIR spectra of 1 mM FBP28 1L in 20 mM potassium phosphate buffer (pH 7). (A) Absorbance spectra in Amide I' region; the temperatures of the individual traces varies from 5 to 85 °C in 5 °C intervals. (B) Difference spectra obtained by subtracting the spectrum at 5 °C from the spectra at higher temperatures.

2. Second derivative spectra of FBP28 1L and 2L absorbance data at 5 °C and FBP28 1L difference data at 33 and 67 °C are taken to determine the subcomponents in the amide I band. The second derivatives were obtained after smoothing the data with a third order (sixth for difference data), binomial algorithm to remove any residual water vapor lines. The data analysis was performed in IGOR PRO (WaveMetrics, Lake Oswego, OR). The individual peaks in the absorbance spectra are more easily distinguished in the second derivative spectra. The second derivative of the absorbance data (Figure 2S) shows three peaks corresponding to secondary structure, centered at 1614, 1638, and 1679 cm^{-1}.

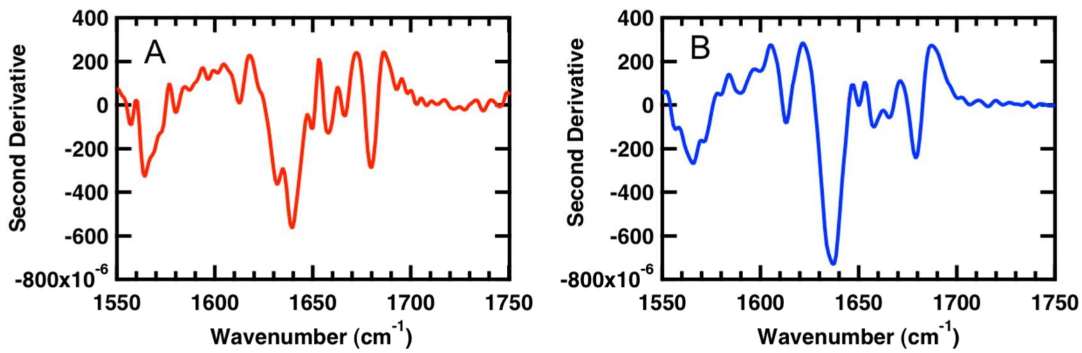

Figure 2S. Second derivative of FTIR absorbance spectrum of FBP28 1L (A) and FBP28 2L (B) at 5 °C.

The second derivatives of the difference spectra at 33 and 67 °C highlight the peaks that are changing with temperature (Figure 3S). At low temperature a peak at 1629 cm^{-1} dominates and at high temperature a peak at 1634 cm^{-1} dominates. The data is normalized to the maximum near 1634 cm^{-1} for comparison.

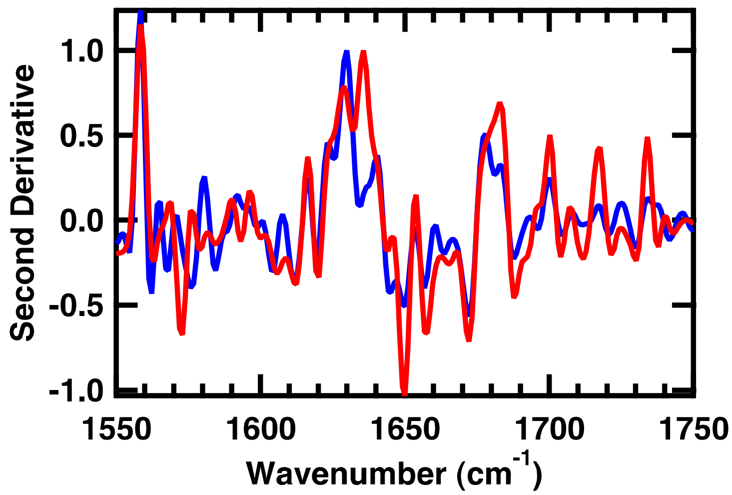

Figure 3S. Second derivative of FTIR difference spectrum of FBP28 1L at 33 (blue) and 67 (red) °C.

3. Temperature dependent infrared T-jump measurements were collected to determine the dynamics of the systems. Please find the IR T-jump method in the methods section of the full paper. Wavelength dependent IR T-jump measurements were collected at 1619 (Table 1S), 1629 (Table 2S) and 1634 cm^{-1} (Table 3S). 15 °C jumps were performed with an initial temperature from 15 to 60 °C. Data reported includes the observed magnitude and relaxation lifetime of each event.

Table 1S: Relaxation Kinetics Probed in the Turn of Loop 1 (1619 cm^{-1}) of FBP28 1L and FBP28 2L

FBP28 1L						
T-jump ΔT(Ti-Tf)/°C	A_1 (mOD)	A_2 (mOD)	A_3 (mOD)	τ_1 (ns)	τ_2 (μs)	τ_3 (μs)
15-30						
20-35						
25-40						
30-45						
35-50						
40-55	1.54±0.03		1.40±0.01	306±11		10.5±0.4
45-60			1.13±0.01			11.9±0.3
50-65	1.63±0.05		0.88±0.01	105±6		8.6±0.5
60-75	1.92±0.01		2.16±0.02	73±9		6.6±0.3
FBP28 2L						
T-jump ΔT(Ti-Tf)/°C	A_1 (mOD)	A_2 (mOD)	A_3 (mOD)	τ_1 (ns)	τ_2 (μs)	τ_3 (μs)
15-30						
20-35						
25-40						
30-45						
35-50						
40-55						
45-60	1.38±0.05	1.44±0.04		131±10	1.83±0.8	
50-65	1.39±0.06	1.70±0.05		185±15	1.7±0.8	
60-75	2.98±0.08	0.79±0.13		135±8	2.7±1.2	

Table 2S: Relaxation Kinetics Probed in the Sheet of WW Domain (1629 cm^{-1}) of FBP28 1L and FBP28 2L

FBP28 1L						
T-jump ΔT(Ti-Tf)/°C	A_1 (mOD)	A_2 (mOD)	A_3 (mOD)	τ_1 (ns)	τ_2 (μs)	τ_3 (μs)
15-30	0.78±0.02	0.96±0.02	0.69±0.01	140±8	2.03±0.06	126±3
20-35	1.06±0.02	1.16±0.01	0.97±0.01	134±5	2.58±0.07	40.8±0.9
25-40	1.02±0.02	1.09±0.01	0.75±0.01	125±5	2.23±0.06	37.6±0.6
30-45	0.96±0.02		0.76±0.01	160±7		28.1±0.9
35-50			2.19±0.01			14.4±0.2
40-55	0.50±0.03		2.45±0.01	178±15		16.3±0.2
45-60		1.21±0.3	1.87±0.31		3.9±0.7	12.4±1.4
50-65		1.29±0.27	3.36±0.12		2.3±0.4	17.2±0.4
60-75			2.74±0.02			15.2±0.4
FBP28 2L						
T-jump ΔT(Ti-Tf)/°C	A_1 (mOD)	A_2 (mOD)	A_3 (mOD)	τ_1 (ns)	τ_2 (μs)	τ_3 (μs)
15-30						
20-35						
25-40	1.52±0.02	1.11±0.02	0.72±0.01	260±8	2.9±0.1	130±5
30-45	1.50±0.03	1.57±0.03	0.60±0.02	203±8	2.48±0.09	43.6±3
35-50	0.70±0.06	1.79±0.10	0.26±0.09	102±17	1.8±0.1	11.3±7
40-55	1.72±0.06	2.49±0.05		157±12	1.74±0.05	
45-60		2.55±0.02			1.79±0.04	
50-65	2.47±0.06	1.22±0.04		213±10	3.1±0.2	
60-75	2.12±0.06	1.64±0.05		152±4	1.7±0.3	

Table 3S: Relaxation Kinetics Probed in the Sheet of Loop 1 (1633 cm^{-1}) of FBP28 1L and FBP28 2L

FBP28 1L						
T-jump ΔT(Ti-Tf)/°C	A_1 (mOD)	A_2 (mOD)	A_3 (mOD)	τ_1 (ns)	τ_2 (μs)	τ_3 (μs)
15-30	0.90±0.03	0.94±0.02	0.66±0.01	163±9	2.12±0.08	140±4
20-35	1.20±0.02	1.19±0.02	1.29±0.01	147±6	2.71±0.09	46.2±0.9
25-40	0.96±0.03	1.26±0.02	1.59±0.02	160±10	2.17±0.09	37.6±0.7
30-45	1.07±0.02	1.27±0.14	1.54±0.14	276±11	8.97±0.83	34.0±2.8
35-50	0.62±0.05		3.09±0.01	62±8		20.6±0.2
40-55	0.85±0.04		4.51±0.01	87±7		14.8±0.1
45-60	0.87±0.08		5.31±0.03	154±24		11.7±0.2
50-65	1.08±0.06		4.27±0.02	151±14		7.9±0.1
60-75	1.37±0.07		3.69±0.03	160±16		4.5±0.1
FBP28 2L						
T-jump ΔT(Ti-Tf)/°C	A_1 (mOD)	A_2 (mOD)	A_3 (mOD)	τ_1 (ns)	τ_2 (μs)	τ_3 (μs)
15-30	1.33±0.03	1.63±0.02	1.04±0.02	117±5	1.52±0.04	250±9
20-35	0.80±0.04	1.17±0.02	1.12±0.24	74±6	1.34±0.04	159±32
25-40	0.77±0.02	1.32±0.01	0.86±0.01	220±12	3.34±0.09	120±4
30-45	1.50±0.03	1.98±0.02	0.81±0.02	169±7	2.69±0.08	44.1±1.9
35-50		1.51±0.06	1.05±0.06		1.34±0.07	11.4±1.1
40-55	1.54±0.07	2.89±0.18	1.13±0.19	106±9	1.69±0.12	7.9±1.3
45-60		3.32±0.02			1.66±0.03	
50-65	2.53±0.09	3.44±0.07		154±11	2.07±0.08	
60-75	5.72±0.18	2.13±0.18		217±12	1.54±0.17	